Microwave-induced elastic deformation of a metallic thin film

2013 J. Phys. D: Appl. Phys. 46 395104

(http://iopscience.iop.org/0022-3727/46/39/395104)

IOP PUBLISHING JOURNAL OF PHYSICS D: APPLIED PHYSICS

J. Phys. D: Appl. Phys. **46** (2013) 395104 (5pp) doi:10.1088/0022-3727/46/39/395104

Microwave-induced elastic deformation of a metallic thin film

S B Wang and C T Chan

Department of Physics and Institute for Advanced Study, The Hong Kong University of Science and Technology, Clear Water Bay, Hong Kong, People's Republic of China

E-mail: phchan@ust.hk

Received 13 June 2013, in final form 4 August 2013
Published 13 September 2013
Online at stacks.iop.org/JPhysD/46/395104

Abstract

The microwave induced elastic deformation of a metallic thin film in a cavity structure is computed using a Maxwell stress tensor method and we found that the microwave can induce a significantly enhanced deformation at the anti-symmetric resonance mode, and the deformation magnitude is a few orders larger than that of the non-resonance case. The previous transmission line approach for the electromagnetic stress (Wang *et al* 2011 *Phys. Rev.* B **84** 075114) is applied to develop an analytical model of deformation based on elastic theory. We show that the analytical model can reproduce the numerical results almost quantitatively and at the same time reveal the underlying physics.

(Some figures may appear in colour only in the online journal)

1. Introduction

Optical force has received a lot of attention and has been applied successfully in recent years in small particle manipulations [1–5]. In a broader sense, electromagnetic induced forces and their ability to manipulate a variety of structures such as tunable metamaterials [6], waveguides [7, 8], nanowires [9, 10] and nanopatches [11–13] have been investigated. However, the effect of stress induced by electromagnetic wave on structures is rarely considered, probably because it is assumed *a priori* that the mechanical effect should be small and hardly detectable (except for soft biological materials [14, 15]), particularly in the microwave regime where it is difficult to focus the microwave onto a small spot with very high intensity due to the diffraction limit. Accurate numerical computation of electromagnetic stress of realistic systems is also fairly involved and previous consideration concerned simple model systems [16]. It is the purpose of this article to explore the microwave-induced stress in a metallic double-film cavity structure, and we show that readily measurable deformation can be induced in very simple settings. Using a Maxwell stress tensor formulation, we determined accurately the form and magnitude of the microwave-induced deformation and we showed that the deformation can be significantly enhanced at the anti-symmetric resonance mode which has a high quality factor. We also showed that the salient features of numerical results can be reproduced analytically using a simple model based on a previously developed transmission line theory [12] which can help to reveal the underlying physics.

2. The metallic double-film structure

We consider a three-dimensional structure consisting of two metallic thin films clamped at the edges by a surrounding dielectric frame ($\varepsilon_r = 2.3$) as shown schematically in figure 1. The two metallic films have a length of a, width of b and thickness of t and they are separated by an air gap of $d = w - 2t$, where w is the thickness of the surrounding dielectric. We will consider the mechanical deformation of the upper film induced by an incident plane wave at the microwave frequency. The incident field has the form:

$$\boldsymbol{E}_{\rm inc} = \hat{x} E_0 \exp[\mathrm{i}(-k_0 z - \omega t)]. \quad (1)$$

The metal is assumed to be gold with a conductivity of $\sigma = 4.098 \times 10^7\,\mathrm{S\,m^{-1}}$.

3. Numerical results and discussions

Photon pressure produced by an incident plane wave on a single metallic film is very weak even at its resonance. However, for the configuration shown in figure 1, the two metallic films (separated by an air gap) form an electromagnetic

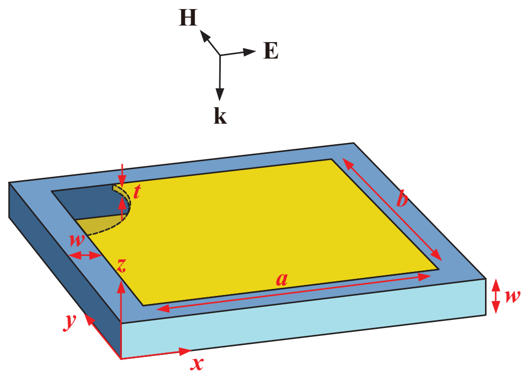

Figure 1. A schematic picture showing the system under consideration. Two metallic films of dimensions $a \times b \times t$ are separated by an air gap and are clamped at the edges by a dielectric frame. The wave vector of the incident plane wave is perpendicular to the surfaces of the metallic films.

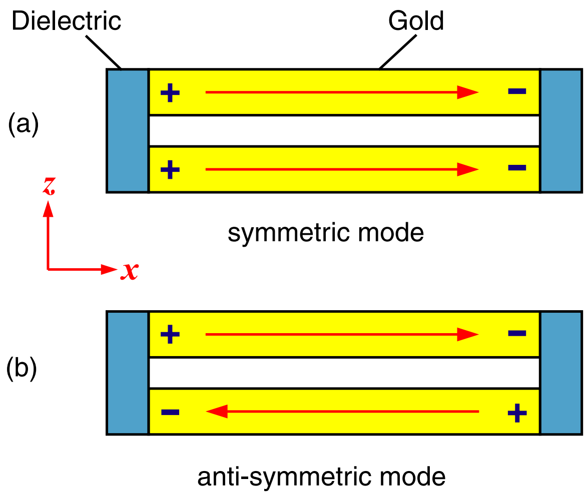

Figure 2. Resonance modes of the metallic double-film structure induced by the incident microwave: (*a*) the symmetric mode is characterized by parallel currents on the surfaces of the films and charges with the same sign at the ends; (*b*) the anti-symmetric mode is characterized by anti-parallel currents on the surfaces of the films and charges with opposite signs at the ends. The arrows show the directions of the induced currents.

cavity [11, 12]. The near-field coupling between the two metallic films will split the resonance into a so-called symmetric/bonding mode and an anti-symmetric/anti-bonding mode (see figure 2) [17]. The symmetric mode is characterized by induced parallel currents on the surfaces of the films and accumulating charges with the same sign at the ends. Such a mode has a relatively low quality factor and we are not interested in it. The anti-symmetric mode has a much higher quality factor as the electromagnetic energy is well confined in the cavity. In the anti-symmetric mode, anti-parallel currents are induced on the surfaces of the two films due to the time-varying electromagnetic flux. The oscillations of the currents produce a non-uniform charge distribution on the films with most of the charges accumulating at the edges along y direction. As a result, we expect the electric field to be strong at the edges while the magnetic field should be strong near the middle of the films. Numerical results shown in figure 3 computed by a finite element package (COMSOL [18]) do verify such a distribution. In the numerical simulations, we set $a = b = 10$ mm, $t = 10\,\mu$m, $w = 120\,\mu$m and we assume a microwave with a total power of 200 mW impinging on the upper surface of the metallic film, which is a plane wave with its wave vector being perpendicular to the metal surface and the electric field being along x-axis (as defined in equation (1)). Figures 3(*d*) and (*e*) show the electric and magnetic fields at the resonance frequency $f = 14.45$ GHz. The electric field between the two films is dominated by the z component, which has opposite directions at the two edges since the accumulated charges have opposite signs. The magnetic field is dominated by the y component, which is strong in the middle region. The red squares in figures 3(*b*) and (*c*) show the numerically computed current and charge distributions, which confirm our previous conclusion. We will show by our analytical model later that the distributions are approximately sinusoidal. The electromagnetic field-induced stress is needed to calculate the elastic deformation of the metallic film. The electromagnetic total fields are first computed, and then the stress is evaluated using the Maxwell stress tensor approach [19]. We note the Maxwell stress tensor approach should not be applied to calculating internal stresses inside a material if the fields penetrate the material [20]. Fortunately, in the microwave regime the penetration depth is negligibly small compared with the thickness of the metal film so that we do not need to worry about the internal stress. In the microwave regime, only the surface stress exerted on the metallic film is important, which can be obtained using the Maxwell stress tensor approach. Figure 4(*a*) shows the distribution pattern of the numerically computed surface stress exerted on the upper film. The stress takes negative values near the edges along y direction while it is positive in the middle region. This corroborates intuitively with the charge and current distributions. At the edges the force is attractive because the accumulated charges have opposite signs. In the middle region the anti-parallel currents produce a repulsive force. This surface stress acts as a boundary load and the deformation caused by the stress is calculated by COMSOL with the clamped boundary condition [21]. Figure 3(*a*) shows the numerically computed maximum deformation of the upper film as a function of the exciting frequency, showing a typical resonance profile. We see that the deformation is strongly enhanced at the resonant frequency 14.45 GHz. Figure 4(*c*) shows the numerically computed deformation pattern of the upper film at 14.45 GHz. The maximum deformation $u_z = 25$ nm happens at the centre point of the film. We note that when the system is off-resonance (e.g. 15.0 GHz), the maximum deformation is only a few angstroms, which is orders of magnitude smaller than the resonance case. This indicates a very strong enhancement due to the field enhancement at the cavity resonance. Even at the resonance, the deformation is still small compared with the air gap between the two films. This is the reason that we can first compute the electromagnetic fields and then apply the corresponding surface stress to calculate the deformation. If a larger microwave power or a much thinner film is employed, the deformation may not be considered as a small perturbation, the electromagnetic part and the elastic part interact with each other and they have to be both considered simultaneously. We

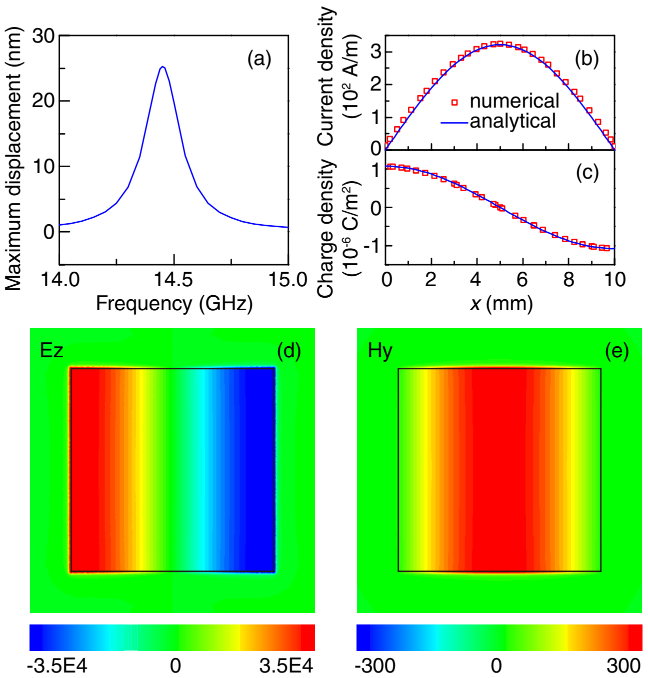

Figure 3. Resonance enhancement of microwave-induced deformation of the metallic thin film structure. (*a*) Maximum displacement of the upper film as a function of the exciting frequency. (*b*) Numerical (squares) and analytical (line) results of the current distribution along *x* direction. (*c*) Numerical (squares) and analytical (line) results of the charge distribution along *x* direction. (*d*) E_z component of the electric total field at resonance on the symmetry plane between the two films showing that the electric field is strongest at the edges. (*e*) H_y component of the magnetic total field at resonance on the symmetry plane between the two films showing the magnetic field is strongest near the centre.

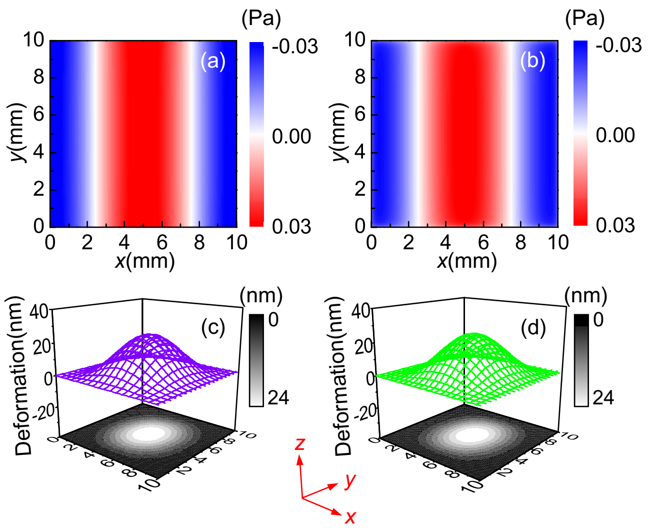

Figure 4. Electromagnetic surface stress and elastic deformation at resonance. (*a*) Electromagnetic surface stress calculated numerically by Maxwell tensor approach. (*b*) Electromagnetic surface stress calculated analytically by the model described in the text. (*c*) Numerical result of the deformation along *z* direction. (*d*) Analytical result of the deformation along *z* direction.

can solve the problem iteratively but for the configuration we are considering, this is not necessary.

4. Analytical model

In the following we show that this problem can be addressed analytically using a model that captures the essence of the physics at this frequency scale. We first obtain the electromagnetic wave-induced stress using a transmission line model [12]. The results given by the model are first briefly summarized (equations (2*a*), (2*b*)–(6)), then we extend the model by elastic theory to calculate the stress-induced deformation. Under the condition $d \ll a$, the two metallic films can be treated approximately as a transmission line where the induced current and voltage are governed by the telegraph equations [22, 23]:

$$\frac{\partial V(x)}{\partial x} + (R - \mathrm{i}\omega L)I(x) = \mathrm{i}\omega\mu_0 \int_{z_1}^{z_2} \hat{y}\cdot \boldsymbol{H}_{\mathrm{inc}}(z)\,\mathrm{d}z, \tag{2a}$$

$$\frac{\partial I(x)}{\partial x} + (G - \mathrm{i}\omega C)V(x) = \mathrm{i}\omega(G + C) \int_{z_1}^{z_2} \hat{z}\cdot \boldsymbol{E}_{\mathrm{inc}}(z)\,\mathrm{d}z, \tag{2b}$$

where $\boldsymbol{H}_{\mathrm{inc}}(z)$ and $\boldsymbol{E}_{\mathrm{inc}}(z)$ are the incident magnetic and electric fields, R is the resistance per unit length, G is the conductance per unit length of the medium sandwiched between the films (zero in this case), $L = \mu_0 d/b$ and $C = \varepsilon_0 b/d$ are the per-unit-length inductance and capacitance of the system, respectively. By applying the resonance boundary condition $I(0) = I(a) = 0$, we can solve the above two equations to obtain the current distribution as

$$I(x) = \frac{B}{A^2}\left[1 - \cos(Ax) - \tan\left(\frac{Aa}{2}\right)\sin(Ax)\right], \tag{3}$$

where

$$A = \sqrt{\omega^2 CL + \mathrm{i}\omega RC}, \tag{4a}$$

$$B = -\mu_0\omega^2 C \int_{z_1}^{z_2} \hat{y}\cdot \boldsymbol{H}_{\mathrm{inc}}(z)\,\mathrm{d}z. \tag{4b}$$

At the microwave frequency we take the limit $R \to 0$ and then the current distribution becomes

$$|I(x)| \approx \left|\frac{B}{A^2}\tan\left(\frac{Aa}{2}\right)\sin(Ax)\right| \tag{5}$$

as the tangent term is dominant at resonance and so the current distribution on the metallic film is approximately sinusoidal. The lowest order resonance frequency is determined by $Aa/2 = \pi/2$, which gives $\omega_0 \approx \pi/(a\sqrt{LC})$. Combining the expressions of L and C we obtain the resonance wavelength $\lambda \approx 2\pi c/\omega = 2a$, which indicates that the resonance frequency here is near the resonance frequency (antenna resonance) of a single film. We note this resonance frequency is valid under the condition $d/a \to 0$. For a finite value of d/a the electric field leakage effect will contribute to an additional capacitance. We take this into account by assigning an effective length to the total capacitance [24], i.e. replace Ca by Ca_{eff} with $a_{\mathrm{eff}} = a(1 + \alpha d/a)$, where α is the coefficient of the first order correction and this correction changes the resonance frequency to

$$\omega_0 \approx \frac{\pi}{a\sqrt{LC(1 + \alpha d/a)}}. \tag{6}$$

By fitting the numerically computed current distribution in figure 3(*b*) we obtain $\alpha = 0.73$. This α is the only parameter in the model and the value is then used throughout our model to calculate the charge distribution and the electromagnetic surface stress. The lines in figures 3(*b*) and (*c*) show the analytical results of current and charge distributions, where the charge distribution is obtained by applying the conservation law of $\nabla \cdot \boldsymbol{j} + \partial\rho/\partial t = 0$. The analytical results agree well with numerical results obtained using full wave electromagnetic field solvers. The electromagnetic surface stress is then obtained by calculating the interaction force point by point between the charges and currents with the Coulomb's law and the Biot–Savart law. Figure 4(*b*) shows the analytically calculated stress distribution, where a good match with the numerical result obtained with Maxwell stress tensor approach is clear.

The elastic deformation of the film is then obtained using elastic theory. The deformation of a thin film under a vertical surface stress can be determined by the equilibrium equation [25]:

$$D\nabla^4 u_z - P(x, y) = 0, \tag{7}$$

where $D = Y_g t^3/[12(1-\nu^3)]$ is the flexural rigidity, $P(x, y)$ is the surface stress/pressure obtained using the transmission line model and $u_z(x, y)$ is the deformation along the z direction. The Young's modulus and the Poisson's ratio of gold are $Y_g = 79$ GPa and $\nu = 0.44$, respectively. The equation is solved by applying the clamped boundary condition:

$$u_z = 0, \quad \frac{\partial u_z}{\partial x} = 0 \qquad \text{at } x = 0, a, \tag{8a}$$

$$u_z = 0, \quad \frac{\partial u_z}{\partial y} = 0 \qquad \text{at } y = 0, b. \tag{8b}$$

In compliance with this boundary condition, we write the trial solution as [21]

$$u_z = \sum_{m=1}^{\infty}\sum_{n=1}^{\infty} C_{mn}\left[1 - \cos\left(\frac{2m\pi x}{a}\right)\right]\left[1 - \cos\left(\frac{2n\pi y}{b}\right)\right]. \tag{9}$$

The coefficients C_{mn} are determined variationally by the Ritz method:

$$\frac{\partial(U - W)}{\partial C_{mn}} = 0, \tag{10}$$

where the strain energy U is

$$U = \frac{D}{2}\iint\left(\frac{\partial^2 u_z}{\partial x^2} + \frac{\partial^2 u_z}{\partial y^2}\right)^2 \mathrm{d}x\,\mathrm{d}y, \tag{11}$$

and the work done by the surface stress is

$$W = \iint P(x, y) u_z \,\mathrm{d}x\,\mathrm{d}y. \tag{12}$$

By truncating the expansion orders at finite values ($m_{\max} = 3$ and $n_{\max} = 3$) we obtain a set of linear equations that can be solved for C_{mn}. Figure 4(*d*) shows the analytical results of the deformation, where an excellent match with the numerical results obtained using brute force simulations is again evident.

5. Conclusions

In conclusion, we have numerically and analytically studied the elastic deformation of a metallic thin film induced by an electromagnetic plane wave at the microwave frequency. We obtained the deformation pattern and showed that the deformation is greatly enhanced at resonance. Deformation on the nanometre scale (maximum value of about 25 nm) is found when utilizing a microwave with 200 mW power incident on the metallic surface. A transmission line model is applied to capture the underlying physics in the electromagnetic part, which almost reproduces the numerical results of electromagnetic surface stress with a fitting fringe effect parameter. A variational method combined with Fourier expansions is then used to calculate the deformation of the metallic thin film, which gives results that match the numerical results very well. It is well established that strong opto-mechanical effects can be observed at optical frequencies and we prove in this paper that microwave can also induce mechanical effects with the help of resonance. The resonance behaviour in our considered structure is very robust and the structure forms a microwave 'drum' that can vibrate under the modulation of the incident wave. We note in particular that a very simple cavity structure can already couple microwave to the mechanical degrees of freedom and this may find applications in the electromagnetic wave manipulations of macro structures in the future.

Acknowledgments

We thank Professors H B Chan and Z Q Zhang for discussions and useful comments and M Yang for the help on COMSOL simulations. This work is supported by Hong Kong CRF grant HKUST2/CRF/11G. S B Wang's studentship is supported by HKUST Nano Science and Technology Programme.

References

[1] Ashkin A 1970 Acceleration and trapping of particles by radiation pressure *Phys. Rev. Lett.* **24** 156
[2] Burns M M, Fournier J M and Golovchenko J A 1989 Optical binding *Phys. Rev. Lett.* **63** 1233
[3] Chu S 1991 Laser manipulation of atoms and particles *Science* **253** 861
[4] Neuman K C and Block S M 2004 Optical trapping *Rev. Sci. Instrum.* **75** 2787
[5] Ng J and Chan C T 2008 Size-selective optical forces for microspheres using evanescent wave excitation of whispering gallery modes *Appl. Phys. Lett.* **92** 251109
[6] Lapine M, Shadrivov I V, Powell D A and Kivshar Y S 2012 Magnetoelastic metamaterials *Nature Mater.* **11** 30
[7] Povinelli M L, Loncar M, Ibanescu M, Smythe E J, Johnson S G, Capasso F and Joannopoulos J D 2005 Evanescent-wave bonding between optical waveguides *Opt. Lett.* **30** 3042
[8] Roels J, De Vlaminck I, Lagae L, Maes B, Van Thourhout D and Baets R 2009 Tunable optical forces between nanophotonic waveguides *Nature Nanotechnol.* **4** 510

[9] Lamothe E, Leveque G and Martin O J F 2007 Optical forces in coupled plasmonic nanosystems: Near field and far field interaction regimes *Opt. Express* **15** 9631

[10] Zhao R K, Tassin P, Koschny T and Soukoulis C M 2010 Optical forces in nanowire pairs and metamaterials *Opt. Express* **18** 25665

[11] Liu H, Ng J, Wang S B, Lin Z F, Hang Z H, Chan C T and Zhu S N 2011 Strong light-induced negative optical pressure arising from kinetic energy of conduction electrons in plasmon-type cavities *Phys. Rev. Lett.* **106** 087401

[12] Wang S B, Ng J, Liu H, Zheng H, Hang Z H and Chan C T 2011 Sizable electromagnetic forces in parallel-plate metallic cavity *Phys. Rev.* B **84** 075114

[13] Zhang J, MacDonald K F and Zheludev N I 2012 Optical gecko toe: optically controlled attractive near-field forces between plasmonic metamaterials and dielectric or metal surfaces *Phys. Rev.* B **85** 205123

[14] Guck J, Ananthakrishnan R, Moon T J, Cunningham C C and Kas J 2000 Optical deformability of soft biological dielectrics *Phys. Rev. Lett.* **84** 5451

[15] Dao M, Lim C T and Suresh S 2003 Mechanics of the human red blood cell deformed by optical tweezers *J. Mech. Phys. Solids* **51** 2259

[16] Sonnleitner M, Ritsch-Marte M and Ritsch H 2012 Optomechanical deformation and strain in elastic dielectrics *New J. Phys.* **14** 103011

[17] Gomez-Medina R and Saenz J J 2004 Unusually strong optical interactions between particles in quasi-one-dimensional geometries *Phys. Rev. Lett.* **93** 243602

[18] COMSOL Multiphysics is a commercial numerical solver for partial differential equations. See, www.comsol.com/

[19] Jackson J D 1999 *Classical Electrodynamics* (New York: Wiley)

[20] Svoboda K and Block S M 1994 Optical trapping of metallic Rayleigh particles *Opt. Lett.* **19** 930

[21] Ugural A C 2009 *Stresses in Beams, Plates, and Shells* 3rd edn (Boca Raton, FL: CRC Press)

[22] Paul C R 2007 *Analysis of Multiconductor Transmission Lines* (Hoboken, NJ: Wiley)

[23] Rachidi F and Tkachenko S 2008 *Electromagnetic Field Interaction with Transmission Lines, from Classical Theory to HF Radiation Effects* (Southampton: WIT Press)

[24] Gupta K C, Garg R, Bahl I and Bhartia P 1996 *Microstrip Lines and Slotlines* (London: Artech House)

[25] Landau L D and Lifshitz E M 1986 *Theory of Elasticity* 3rd edn (Oxford: Pergamon)